

M. MÜLLER<sup>1,✉</sup>  
B. MURPHY<sup>1</sup>  
M. BURGHAMMER<sup>2</sup>  
I. SNIGIREVA<sup>2</sup>  
C. RIEKEL<sup>2</sup>  
J. GUNNEWEG<sup>3</sup>  
E. PANTOS<sup>4</sup>

# Identification of single archaeological textile fibres from the cave of letters using synchrotron radiation microbeam diffraction and microfluorescence

<sup>1</sup> Institut für Experimentelle und Angewandte Physik der Christian-Albrechts-Universität zu Kiel, Leibnizstr. 19, 24098 Kiel, Germany

<sup>2</sup> European Synchrotron Radiation Facility, B. P. 220, 38043 Grenoble Cedex, France

<sup>3</sup> Institute of Archaeology, The Hebrew University of Jerusalem, Mount Scopus, Jerusalem, Israel

<sup>4</sup> Daresbury Laboratory, Keckwick Lane, Warrington WA4 4AD, UK

Received: 5 December 2005 / Accepted: 10 December 2005  
© Springer-Verlag 2006

**ABSTRACT** Single 2000-year-old archaeological fibres from textile fragments excavated in the Cave of Letters in the Dead Sea region were investigated by a combined approach using microscopy (optical and SEM), X-ray microbeam diffraction and X-ray microbeam fluorescence. In comparison with modern reference samples, most of the fibres were identified as wool, some as plant bast fibres (flax). The molecular and supermolecular structure of both keratin (wool) and cellulose (flax) were found completely intact. In many fibres, mineral crystals were intimately connected with the fibres. The fluorescence analysis of the dyed wool textiles suggests the possible use of metal-containing mordants for the fixation of organic dyes.

**PACS** 61.10.Nz; 78.70.En; 81.05.Lg

## 1 Introduction

The aim of the experiments was to identify textile fibres found in the “Cave of Letters” in the Dead Sea region. The Cave of Letters (hence CoL) is called so because of the finding of the Bar Kochba (last freedom fighter) letters there, dating from the second revolt of the Jews against the Romans around 135 AD. The cave is located on the northern cliff-face of Nahal Hever and is some 150 meters long. The last hiding Jews used the cave, which is located about three kilometers west of the Dead Sea, as a habitat. The CoL textiles are unique of second century AD only. Wool, linen and all kinds of garments were found, sometimes even near-complete tunics. From the archaeological point of view, the study of these textiles is without any doubt of great importance for determining what the Romans and the Jews wore in the second century AD in the eastern Mediterranean and where they got their materials from.

The cliffs where the CoL is located are the continuation of the Qumran cliffs. Textiles from the caves of Qumran have been previously investigated with synchrotron radiation [1, 2]. The use of single fibres avoided artefacts from fibre bundles. The microdiffraction results obtained, com-

plemented classical microscopic investigations (optical and scanning electron microscopy, SEM) and standard X-ray diffraction. A focussed synchrotron radiation X-ray beam with a high flux density can be used to collect diffraction diagrams of single fibres of a weakly scattering material like cellulose or wool within a few seconds [3–5]. The study could clearly distinguish between wool and plant fibres and even between different kinds of plant bast fibres. It led to the unambiguous identification of flax (linen) and – most unexpectedly for archaeologists – cotton textiles. (The latter, however, received later dates after AMS C14 was applied [6].)

An attempt to identify the nature of the fibres in the CoL textiles by Raman spectroscopy has been hampered by the degradation of the fibres. Thus, we used the same combination of techniques, supplemented by X-ray fluorescence spectroscopy, as in our previous study of similarly degraded fibres from Qumran (cave 11Q and the Christmas Cave) [1, 2] for the analysis of the CoL textiles presented here.

Unlike the textiles from Qumran, most of those found in the Cave of Letters are dyed. Pigments and solid particles attached to the samples can be identified unambiguously by their diffraction pattern (if they are sufficiently ordered) or by their elemental composition. Hence, in this study fluorescence spectra were additionally recorded simultaneously with diffraction images, thus providing complementary information at the same time, at the same location on the fibre and with the same spatial resolution.

## 2 Experimental details

Nine different textile samples were selected at the Hebrew University from a collection that was found in the Cave of Letters, Locus 2, HH41 B 166. Inspection under a stereo-microscope has shown all of them to be *S*-spun (left-handed), which is normally typical for bast fibre handedness whereas wool is usually *Z*-spun (right handed). The samples were untreated and thus contained soil particles.

Only two textile fragments, CoL 205 and CoL 208, show their native colour, a very light brown or yellow, almost white. Their colour is indicative of a plant origin. The fragments CoL 201 and CoL 204 are of a bright red colour, CoL 207 and CoL 209 are dark red or brown. The threads of the samples CoL

✉ Fax: +49-(0)431-880-1685, E-mail: mmueller@physik.uni-kiel.de

name	type	colour	Si	P	S	Cl	K	Ca	Ti	V	Cr	Mn	Fe	Ni	Cu	Zn	Pb
201	wool	bright red	o	o	++		+	++	+	o	o	+	++		+	+	+
204	wool	bright red		+	++	++	++	++	o			o	++		+	+	
207	wool	brown	o	o	++	++	++	++	+	o		+	++			o	
209	wool	brown		o	++	++	++	++	+	o		+	++		o	o	
210a	wool	brown	o	o	++	++	++	++	+	o		o	++		o	o	
202	wool	dark blue			++		o	++	+				++		+	+	
210bd	wool	dark blue			++	++	++	++	o			o	+		o	+	
210bl	wool	light blue	o	o	++	+	+	++	+	o	o	+	++		++	+	
203	wool	black	o	o	++	++	++	++	+	o	o	+	++	o	+	+	
205	flax	native	o		o	++	++	++	+			o	++			+	
208	flax	native					o	++					++		o	+	
flax	bast	bleached						++				o	+				
linen	bast	bleached						+							o	+	
jute	bast	native					+	+	o				+				
ramie	bast	bleached					+	o									
ramie	bast	native						+	o				+				

**TABLE 1** Overview of results of microscopy, microdiffraction and microfluorescence on archaeological fibres (sample names CoL + name in table) and modern reference samples. The symbols in the elemental distribution columns mean very strong (++) or strong (+) fluorescence lines or traces (o). No symbol indicates that this element could not be detected

202 and CoL 203 are dyed in very dark colours: CoL 203 is almost black, CoL 202 is intense blue. Sample CoL 210 contains separate textile threads of three different colours. In the present paper, we use the acronym CoL 210a for brown fibres, CoL 210bd for dark blue ones (similar to CoL 202) and CoL 210bl for those of a light though intense blue. Modern plant bast fibres (flax, jute and ramie) were investigated as references. Table 1 gives an overview on the 16 different fibres investigated in this study.

Individual fibres of a few millimeters length were carefully extracted from the samples using tweezers under a stereo-microscope. Handling of the archaeological fibres was more difficult than for modern fibres since the material was much more brittle, indicating a certain degree of degradation. Fibre diameter was typically between 10 and 20  $\mu\text{m}$ . For scanning electron microscopy (SEM) investigations, a thin (10–20 nm) film of gold was cast onto the samples. For the X-ray experiments, several different single fibres were mounted on a single U-shaped plastic frame (open to one side) for increased efficiency of the microdiffraction experiment. The fibres were oriented vertically. The sample holder was mounted on a motorised goniometer head.

Diffraction patterns and fluorescence spectra were collected at the Microfocus Beamline ID13 at the European Synchrotron Radiation Facility (ESRF, Grenoble, France) [7]. X-rays of 0.0976 nm wavelength (energy 12.7 keV) were used in the experiment. The synchrotron radiation was focused to a circular spot of 2  $\mu\text{m}$  in diameter using Kirkpatrick-Baez mirrors and a tapered glass capillary. The incident beam intensity was monitored with an ionisation chamber in front of the sample. A Pt/Ir aperture placed 1.5 mm before the sample removed most of the X-ray background from the beam path further upstream. The sample holder was scanned through the microbeam with accuracy better than 1  $\mu\text{m}$ . In an automated scan all single fibre samples of one frame were subsequently scanned in three horizontal lines, separated vertically by 10  $\mu\text{m}$ , in 16 steps of 5  $\mu\text{m}$ . Acquisition time was about 10 s per step, depending on the actual time to reach 2 500 000 monitor counts. Two-dimensional diffraction patterns were recorded on a MAR CCD detector with 64.45  $\mu\text{m} \times 64.45 \mu\text{m}$

pixel size. The sample-detector distance was calibrated with a corundum standard and was approximately 102 mm.

Microbeam X-ray fluorescence spectra [8] were simultaneously acquired using a very compact, high counting rate detector (Röntec XFlash) in about 5 mm distance from the beam position. X-ray fluorescence radiation emitted under about 90° and in the direction of the open side of the sample holder frame could directly pass to the detector window. As the scans described above were always wider than the fibre diameter, background spectra were obtained as well. They were mainly contaminated by platinum and iridium fluorescence lines (originating from the last aperture in the beam, around 9.5 keV) and that of argon (from the air path, around 3 keV). The usable spectral range was between 1.5 and 11 keV.

The ESRF image processing software FIT2D [9] was used for analysis of the two-dimensional diffraction patterns (e.g., averaging, azimuthal integration; see below).

SEM images of the samples were obtained with a LEO 1530 microscope (20 kV) in the ESRF Microimaging and Micromanipulation Laboratory.

### 3 Results and discussion

#### 3.1 Microscopy (optical and SEM)

The textile samples from the Cave of Letters show almost no signs of degradation in the optical microscope. Practically all individual fibres in a single thread remained intact after nearly 2000 years in the sediment of the caves. As already mentioned in the previous section, the mechanical properties of the fibres, in particular the pronounced brittleness, indicate some internal degradation of the fibre material. The colours of the textiles are very bright and intense and thus probably still close to their initial state when the garments were worn.

Some of the fibres can readily be identified as wool by their very regular outer shape and the high transparency of the homogenous fibre material. The uncoloured fibres CoL 205 and CoL 208 are very probably plant fibres. The bright red sample CoL 204 is an example of a far more difficult identification, and required further inspection with higher resolution (SEM).

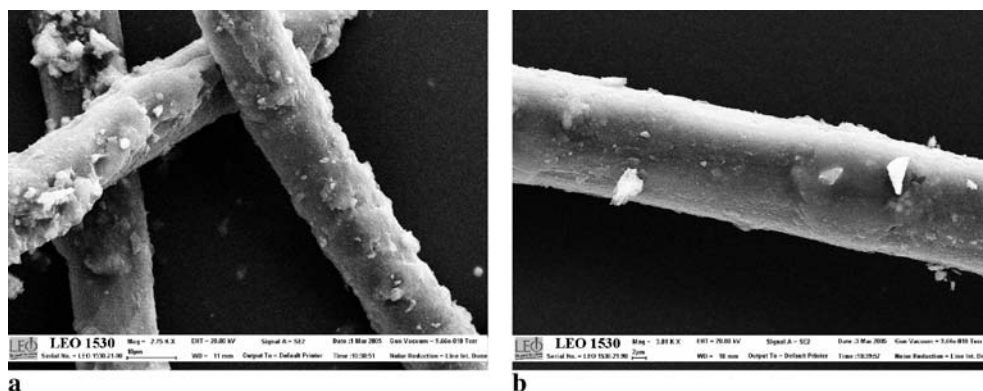


**FIGURE 1** Scanning electron microscopy (SEM) images of archaeological fibres. (a) Sample CoL 204, magnification 2750 $\times$ , scale bar 10  $\mu\text{m}$ , diameter of rightmost fibre 16.2  $\mu\text{m}$ , fibre type identified as wool by X-ray microdiffraction; (b) sample CoL 205, magnification 3810 $\times$ , scale bar 2  $\mu\text{m}$ , fibre diameter 16.6  $\mu\text{m}$ , preliminary identification as bast fibre confirmed by X-ray microdiffraction (flax)

Exemplary SEM images of single fibres from textile fragments CoL 204 and CoL 205 are shown in Fig. 1. The plant fibre CoL 205 has a smooth surface and shows (in the right half of the image) the hint of a typical dislocation (“knee” defect) as found in bast fibres, in particular in flax [10] (Fig. 1b). More pronounced “knees” were seen in SEM images of other fibres of this sample. The fibre has a diameter of 16.6  $\mu\text{m}$  which is a very typical value again for flax [3, 10]. CoL 204 exhibits a much more rugged surface of fibres with a very similar diameter (Fig. 1a; rightmost fibre: 16.2  $\mu\text{m}$ ). This surface morphology could mean a further state of degradation as compared to CoL 205 or a completely different fibre type like wool. However, even though defects along the fibres are not present in these fibres there are no distinct features allowing unambiguous identification of CoL 204. It was only possible with X-ray microdiffraction (see Sect. 3.2 below).

Some of the SEM images of fibres already identified as wool with the optical microscope clearly show the scale-like periodic structure of the wool fibre cuticula.

The SEM images reveal another very important feature of the ancient samples. Not only is the fibre surface covered with microscopic and sub-microscopic soil particles as expected from finding the textile fragments in the cave sediments, but there seem to be aggregates of non-fibrous, probably inorganic material intimately connected with the fibre surface (Fig. 1a). For fibres in these conditions further cleaning procedures, e.g. washing in distilled water or mild solvent, are thus not considered very promising.

### 3.2 X-ray microbeam diffraction

The diffraction diagrams obtained from single fibres made the distinction between fibres of plant and animal origin readily possible. Only two general types of diffraction patterns were found. Examples of both types are shown in Fig. 2: CoL 204 in Fig. 2a and CoL 205 in 2b (thus, the same samples as in Fig. 1). At first glance, two different species of peaks are discernible in all diffractograms: larger ones with strong radial broadening and with well-defined arcing on the azimuth, originating from the fibre material, and sharp reflections on ill-defined incomplete powder Debye-Scherrer rings. The latter are very probably from the inorganic crystals that were already visible in the SEM images (Fig. 1). Consequently, the highly encrusted fibre CoL 204 shows far more mineral contribution than CoL 205 with only a few particles attached to the fibre.

The broader peaks in the diffraction diagrams are from the fibre material itself. The inherent fibre texture, with all molecules essentially aligned parallel to the longitudinal fibre axis, leads to a so-called fibre diagram. With fibres oriented vertically as in the experiments presented here, the equator of the fibre diagram is oriented horizontally, the meridian vertically.

Figure 2a from sample CoL 204 which posed identification problems with microscopic techniques (see above) exhibits all expected features of X-ray diffraction from wool [11]. Wool fibres are well-ordered on longer length scales and thus display diffraction spots mainly in the small-

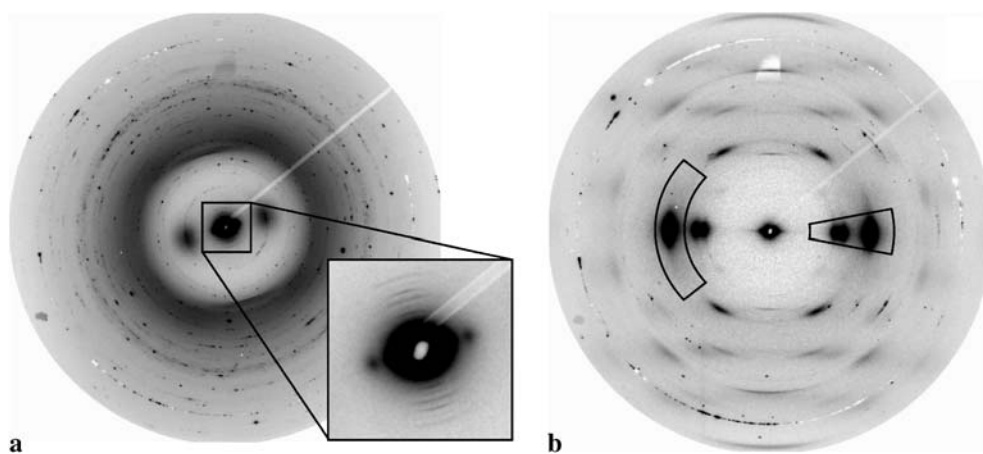


**FIGURE 2** X-ray microdiffraction diagrams of single fibres from samples (a) CoL 204 and (b) CoL 205 (2  $\mu\text{m}$  beam size, ca. 10 s acquisition time). (a) The more diffuse reflections in the diagram have fibre symmetry and are typical of wool (keratin). The inset magnifies the small-angle region, again with reflection attributed to keratin. The sharper reflections on incomplete powder (Debye-Scherrer) rings originate from small mineral crystals. (b) Typical fibre diffraction diagram of a highly oriented cellulose bast fibre (flax). The lines indicate the areas used for integration of data to yield one-dimensional scans (see Fig. 3)

angle region (see inset of Fig. 2a). In contrast, the diffraction pattern of CoL 205 is a perfect match of a fibre pattern of well-oriented cellulose [4]. The clearly visible Bragg peaks up to higher orders reflect the crystalline order of the cellulose molecules in the fibre. – Only the undyed threads of CoL 205 and CoL 208 are identified as cellulose fibres of plant origin, all other textiles were dyed and made from wool (see Table 1).

In the following, we will discuss in detail the features of wool fibres, cellulose fibres and mineral crystals separately.

**3.2.1 Wool fibres.** Wool mainly consists of the fibrous protein  $\alpha$ -keratin whose architecture is based on  $\alpha$ -helices oriented parallel to the fibre axis. The two-dimensional diffraction pattern of a single fibre of the sample CoL 204 (Fig. 2a) is typical for keratin. The sharp lines of the meridian indicate the 0.515 nm helix pitch projection, the diffuse equatorial peaks (just outside the square in Fig. 2a) the 0.98 nm distance between helix axes [11]. Furthermore, the supermolecular structure is also intact as shown in the inset (zoom into the small-angle region of the diffraction diagram): the well-defined equatorial reflections correspond to a characteristic 8.8 nm distance of the packing of keratin protofibrils into filaments [12], several orders of sharp meridional reflections indicate a periodic morphology along the fibre axis.

In summary, the molecular and supermolecular structure of wool was preserved during the two millennia that the CoL textiles have been lying in the sediments of the cave. Similarly well-preserved structures of keratin have also been found in the hair of ancient Egyptian mummies of about the same age [13].

**3.2.2 Cellulose fibres.** Cellulose is a semi-crystalline material with small cellulose crystallites (typically 4–7 nm in diameter), so-called microfibrils, embedded in an amorphous matrix. Figure 2b (single fibre of sample CoL 205) is a very typical fibre diffraction diagram of cellulose fibres with high orientational order [4]. The three strongest cellulose reflections  $1\bar{1}0$ ,  $110$  and  $200$  (from the beam centre;  $200$  is strongest) are found on the equator of the diagram [14].

The orientational properties of the cellulose microfibrils can in principle be seen directly from the raw data where the azimuthal arcing (broadening) of the Bragg reflections is a direct measure for the internal orientation of the cellulose. Bast textile fibres like flax, hemp, jute or ramie are characterised

by a very high orientation of the cellulose microfibrils along the direction of the fibre axis. For a quantitative analysis, the area of the CoL 205 pattern around the  $200$  reflection as indicated in Fig. 2b (left of beam centre) was integrated radially to yield an azimuthal scan, shown in Fig. 3b (dashed line). For CoL 208 (dash-dotted line), its width and even the overall profile of the curve coincide perfectly with that of a modern flax fibre (continuous line). The orientation of CoL 205 (dashed line) is slightly worse, however, still close enough to conclude for those two fibres that flax is the most probable material. The match with the other reference bast fibres (ramie, jute) is much worse.

To corroborate these findings, the radial equatorial intensity profiles were also compared. The fibre diagrams were azimuthally averaged in an angular region of about 20 degrees around the equator (see area indicated in Fig. 2b, right of beam centre). The radial width of the relatively broad equatorial reflections contains information about the cross section dimension of the cellulose microfibrils, which is specific for a given plant species [15]. The thus obtained one-dimensional diffraction curves (Fig. 3a) contain just the three reflections mentioned above in the range of the wave vector transfer  $Q = (4\pi/\lambda) \sin \Theta$  (scattering angle  $2\Theta$ ) from 0.5 to  $2.1 \text{ \AA}^{-1}$ . Again, we find a perfect match of the CoL 208 data and a slightly worse coincidence of the CoL 205 curve with modern flax. However, since the peak widths are practically identical, the identification of CoL 205 and CoL 208 is unambiguous.

One reason for the small differences between the diffraction curves of modern flax and of CoL 205 could be a different content of amorphous material. This should give rise to a very broad background peak centred at about  $1.49 \text{ \AA}^{-1}$  [16]. A small variation of the background intensity would change details of the intensity profile. A change of the amount of amorphous material, in particular a loss of it due to aging of the archaeological fibre, could also explain the brittleness of the ancient fibres as the amorphous material forms the soft matrix of the composite material cellulose. The cellulose microfibrils are much harder than the entire fibre [17] and do not have the fibre's flexibility.

Apart from these small details, the CoL linen textiles are remarkably well preserved in the sense that their crystalline parameters and properties vary little from those of modern samples taken for comparison. This is in agreement with the

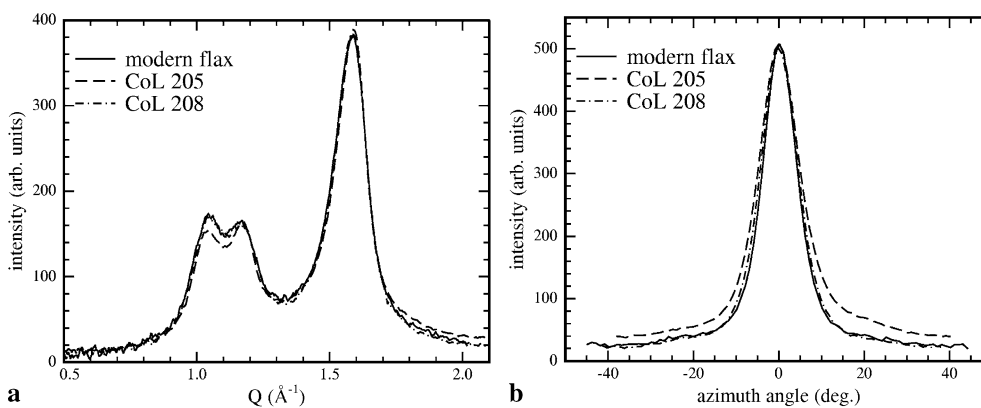


**FIGURE 3** Radial (a) and azimuthal (b) intensity distributions of the two-dimensional diffraction diagram of CoL 205 (Fig. 2b), obtained by respective integration of the areas indicated in Fig. 2b. Both CoL 205 and 208 match the corresponding data of modern flax very well

previously investigated textiles from Qumran of about the same age [1, 2].

**3.2.3 Mineral crystals.** Some of the diffraction diagrams with a very high contamination by diffraction rings from inorganic crystals were integrated over the azimuth angle to yield one-dimensional diffraction diagrams. However, a reliable powder averaging is impossible. There is no powder texture on the length scale of the micrometer beam size but the powder grains are larger than or of the order of the beam size. Consequently, the Bragg intensities cannot be used for phase analysis of the inorganic crystals; only the peak positions can be used for the identification of minerals. As an example, the analysis of the diffraction of CoL 201a yielded significant contributions of quartz, kaolinite, calcite and biotite. A number of peaks remained unidentified. The complex mixture of minerals is consistent with geological and mineralogical investigations of the sediments in the Cave of the Letters [18].

### 3.3 X-ray microbeam fluorescence

Examples of the obtained fluorescence spectra are shown in Fig. 4. The spectra of one scan across the single fibre were averaged. The pronounced double peaks of calcium ( $K\alpha$  energy 3.690 keV) and iron ( $K\alpha$  energy 6.397 keV) are present in all spectra and were used for internal energy calibration. Around 3 keV and 9.5 keV there are artefact visible due to background subtraction (see Experimental Details section). The energies of fluorescence lines of all elements found are given by dotted lines in the plot. The complete results are given in Table 1. Very strong fluorescence is marked by ++ (e.g. the Ca lines in the spectra of Fig. 4) and a strong contribution by + (e.g. Zn in the spectrum of CoL 210bd in Fig. 4). If only traces are found, like for example Cu in CoL 201bd, see Fig. 4), this is indicated by an open circle. No symbol means the absence of fluorescence lines of the respective element.

The elemental distribution is very similar among all fibres found in the Cave of the Letters. This finding is irrespective of the colour of the specific fibres. In contrast, the modern reference fibres contain mostly only Ca and Fe. In conjunction with the presence of minerals as seen in the diffraction patterns we thus conclude that the fluorescence spectra of the CoL textiles mainly constitute a fingerprint of the soil composition in the cave's sediment.

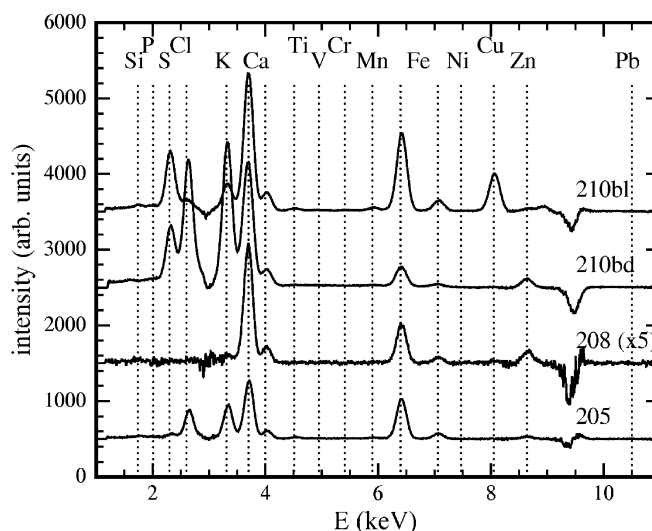


**FIGURE 4** X-ray fluorescence data obtained with a 2  $\mu\text{m}$  wide microbeam, averaged over the fibre diameter of single wool fibres (CoL 210bd and 210bl) and flax fibres (CoL 205 and 208). Negative peaks and/or noise around 3 keV and 9.5 keV are artefacts from background subtraction

There are only very few special cases that require a more detailed investigation. Additional information about the location of a specific element in a fibre or at its surface is found in the position resolved spectra, yielding local elemental distribution maps. Figure 5 shows those maps of samples CoL 210bd (Fig. 5a) and of CoL 210bl for some selected elements.

The presence of sulphur in all wool fibres is easily understood. The main structural material in wool or hair is the fibrous protein keratin, which contains sulphur in the amino acid cystine. For the interpretation of Fig. 5 we thus assumed that the S intensity in a scan across a single wool fibre (dashed lines) reflects the volume function of the fibre, i.e. the amount of material in the beam.

Some of the other elements deviate strongly from the S distribution, in particular Ca in the CoL 210bd fibre (Fig. 5a) and Fe in the CoL 210bl fibre. The sharp pronounced peaks coincide with very intense diffraction rings and are very likely due to mineral grains adhering to the fibre surface. The combined analysis of fluorescence and diffraction data for mineral phase identification is still in progress.

The only remaining candidates for elements associated with the dyeing process of the wool are those with a more ho-

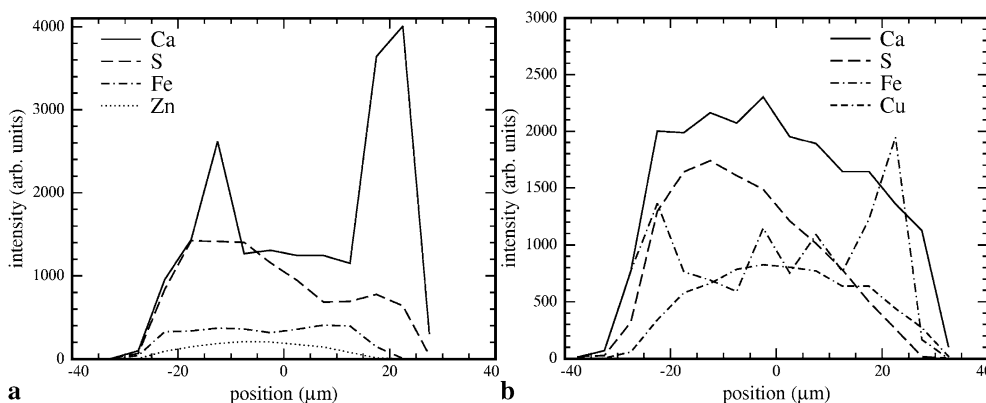


**FIGURE 5** Results of microfluorescence scans across single fibres of (a) CoL 210bd and (b) CoL 210bl. Data correspond to intensities of fluorescence line of the respective elements

mogeneous local distribution like Zn for CoL 510bd and Cu for CoL 510bl. Moreover, zinc and copper are not present in equal amounts in all CoL samples and thus do not have to be considered as “fingerprint” elements of the soil. At this stage, we can only speculate about the relation of Cu and Zn with fibre dyeing. Organic dyes are usually used with so-called mordants, solutions of metals salts used to fix natural dyes to fabric [19]. The material to be dyed is first “mordanted” in the chosen metal salt, by heating it in water with the mordant. Then it is transferred to the dye bath and again heated for a permanent, rich colour. Different mordants usually produce different colours from the dye [19]. If Zn and Cu in the two CoL 210b samples were mordant-related that could explain the different intensities of their blue colours.

#### 4 Conclusions

The study on archaeological textiles from the Cave of Letters presented here is (after similar investigations on textiles from Qumran [1, 2]) another successful example for the use of X-ray microbeam techniques in archaeometry. In particular, these experiments would not have been possible without the use of synchrotron radiation.

Single fibres have been precisely identified, even those where optical microscopy and SEM images alone did not allow identification. Most of the textiles found in the CoL were made from wool (dyed in intense colours) and only a few from linen (native undyed flax fibres). This finding is very interesting in the archaeological context and is in contrast to the results on textiles from Qumran (mostly undyed linen [1, 2]), indicating a significantly different cultural background of the people using the respective textiles.

The internal structure of the fibres on the molecular and supermolecular level turned out to be extremely well preserved after two millennia in the cave sediments.

Many questions have been answered, which has in turn given rise to new a curiosity. There remain some open questions regarding dyes and soil particles. The latter display

a very complex phase mixture of different minerals, which are sometimes intimately connected with the fibres. Concerning the dyed wool fibres, some of them show a high internal concentration of copper or zinc. One possible explanation is that metal salts were used as mordants helping in the process of dyeing with organic substances. Further investigation of the dyes is planned using optical spectroscopic methods.

#### REFERENCES

- 1 M. Müller, M.Z. Papiz, D.T. Clarke, M.A. Roberts, B.M. Murphy, M. Burghammer, C. Riekkel, E. Pantos, J. Gunneweg, in: J.-B. Humbert, J. Gunneweg (Eds.) *Archaeological Excavations at Khirbet Qumran and Ain Feshka – Studies in Archaeometry and Anthropology*, Vol. II, Chapt. XII, pp. 177–186 (Presses Universitaires de Fribourg, Suisse, 2003)
- 2 M. Müller, B. Murphy, M. Burghammer, C. Riekkel, M. Roberts, M. Papiz, D. Clarke, J. Gunneweg, E. Pantos, *Spectrochim. Acta B* **59**, 1669 (2004)
- 3 M. Müller, C. Czihak, G. Vogl, P. Fratzl, H. Schober, C. Riekkel, *Macromolecules* **31**, 3953 (1998)
- 4 M. Müller, C. Czihak, M. Burghammer, C. Riekkel, *J. Appl. Cryst.* **33**, 817 (2000)
- 5 L. Kreplak, C. Mérigoux, F. Briki, D. Flot, J. Doucet, *Biochim. Biophys. Acta* **1547**, 268 (2001)
- 6 Proc. of the Cost Action G8 Working Group 7 Qumran Meeting, Jerusalem, 22 & 23 May 2005, to be published
- 7 C. Riekkel, *Rep. Prog. Phys.* **63**, 233 (2000)
- 8 A. Berglund, H. Brelid, A. Rindby, P. Engström, *Holzforschung* **53**, 474 (1999)
- 9 A.P. Hammersley, S.O. Svensson, A. Thompson, *Nucl. Instrum. Methods A* **346**, 312 (1994)
- 10 A. Satta, R. Hagege, M. Sotton, *Bull. Sci. ITF* **15**, 3 (1986)
- 11 F. Briki, J. Doucet, C. Etchebest, *Biophys. J.* **83**, 1774 (2002)
- 12 F. Briki, B. Busson, J. Doucet, *Biochim. Biophys. Acta* **1429**, 57 (1998)
- 13 L. Bertrand, J. Doucet, P. Dumas, A. Simionovici, G. Tsoucaris, P. Walter, *J. Synchrotron Radiat.* **10**, 387 (2003)
- 14 C. Woodcock, A. Sarko, *Macromolecules* **13**, 1183 (1980)
- 15 A.C. O’Sullivan, *Cellulose* **4**, 173 (1997)
- 16 A. Isogai, R.H. Atalla, *Polym. Sci. Polym. Chem.* **29**, 113 (1991)
- 17 A. Ishikawa, T. Okano, J. Sugiyama, *Polymer* **38**, 463 (1997)
- 18 A. Frumkin, *J. Geol.* **109**, 79 (2001)
- 19 H. Schweppe, *Handbuch der Naturfarbstoffe* (Nikol Verlagsges., Hamburg, 2001)